ELSEVIER

Signal Processing 80 (2000) 1883–1894

SIGNAL PROCESSING

www.elsevier.nl/locate/sigpro

Identification of a neuroelectric system involving a single input and a single output

A.G. Rigas[a], P. Liatsis[b,*]

[a]*Department of Electrical and Computer Engineering, Democritus University of Thrace, GR-67100 Xanthi, Greece*
[b]*Intelligent Systems and Sensing Laboratory, Control Systems Centre, Department of Electrical Engineering and Electronics, UMIST, Sackville Street, P.O. Box 88, Manchester M60 1QD, UK*

Received 2 September 1999; received in revised form 2 March 2000

Abstract

In this work, we identify a neuroelectric system by using a stochastic model of Volterra type. The neuroelectric system is called muscle spindle and plays a critical role in the initiation of movement and in the maintenance of posture. In order to identify the stochastic model we use spectral analysis techniques of stationary point processes, which are based on Welch's method. New asymptotic results for the gain, phase and impulse function of the system based on the Welch's method are obtained. These results are used in examining the behaviour of the muscle spindle under two different experimental conditions: (a) when there is no input present and (b) when an input is present. The presence of the input drastically modifies the behaviour of the muscle spindle. It is shown from the estimates of the gain and phase that the system behaves as a high-pass filter with the input leading the output by about 30 ms. This result is also verified from the estimate of the impulse function which indicates that the system does not respond for about 30 ms. © 2000 Elsevier Science B.V. All rights reserved.

Zusammenfassung

In dieser Arbeit identifizieren wir ein neuroelektrisches System durch Verwendung eines stochastischen Volterramodells. Das neuroelektrische System wird Muskelspindel genannt und spielt eine kritische Rolle bei der Einleitung einer Bewegung und bei der Aufrechterhaltung der Körperhaltung. Um das stochastische Modell zu identifizieren, verwenden wir Methoden der Spektralanalyse für stationäre Punktprozesse, die auf der Welch-Methode beruhen. Es werden neue Resultate für die Verstärkungs-, Phasen- und Impulsfunktion des auf der Welch-Methode basierenden Systems erzielt. Diese Ergebnisse werden bei der Untersuchung des Verhaltens der Muskelspindel unter zwei unterschiedlichen Versuchsbedingungen benutzt: (a) wenn kein Eingangssignal vorliegt und (b) wenn ein Eingangssignal vorliegt. Das Verhalten der Muskelspindel wird durch die Präsenz eines Eingangssignals drastisch verändert. Anhand der Schätzung der Verstärkung und der Phase wird gezeigt, dass sich das System wie ein Hochpassfilter verhält, wobei das Eingangssignal dem Ausgangssignal um etwa 30 msec vorausgeht. Diese Ergebnis wird ebenfalls durch die Schätzung der Impulsfunktion verifiziert, die anzeigt, dass das System 30 ms lang nicht antwortet. © 2000 Elsevier Science B.V. All rights reserved.

Résumé

Nous identifions dans ce travail un système neuro-électrique à l'aide d'un modèle stochastique de type Volterra. Le système neuro-électrique est appelé le fuseau musculaire et joue un rôle critique dans l'initiation du mouvement et la

* Corresponding author: Tel: + 44-161-200 4659; fax: + 44-161-200 4647.
E-mail address: p.liatsis@umist.ac.uk (P. Liatsis).

PII: S0165-1684(00)00095-5

maintenance de la posture. Nous utilisons des techniques d'analyse spectrale de processus ponctuels stationnaires, basées sur la méthode de Welch, pour identifier le modèle stochastique. Nous obtenons des résultats asymptotiques nouveaux sur le gain, la phase et la réponse impulsionnelle du système sur la base de la méthode de Welch. Ces résultats sont utilisés pour examiner le comportement du fuseau musculaire dans deux conditions expérimentales différentes: (a) quand aucune entrée n'est présente et (b) quand une entrée est présente. La présence d'une entrée modifie drastiquement le comportement du fuseau musculaire. Il est montré à partir des estimées du gain et de la phase que le système se comporte comme un filtre passe-haut présentant un retard d'environ 30 ms. Ce résultat est également vérifié par le biais de l'estimée de la répons impulsionnelle, qui indique que le système ne répond pas pendant environ 30 ms.

Keywords: Stationary point processes; Spectral analysis; Welch's method; System identification; Neuroelectric system

Nomenclature

p_k	mean intensity	$\hat{d}_k(\lambda, j)$	modified Fourier–Stieltjes transform
$p_{k\ell}(u)$	second-order product density	$\hat{I}_{k\ell}(\lambda, j)$	modified periodogram
$q_{k\ell}(u)$	cumulant density	$a(u)$	impulse response function
$f_{k\ell}(\lambda)$	spectral density function	μ	mean rate of process
$\lvert R_{k\ell}(\lambda)\rvert^2$	coherence coefficient	$A(\lambda)$	transfer function
		$\log_{10}\lvert A(\lambda)\rvert$	gain of transfer function
		$\theta(\lambda)$	phase of transfer function

1. Introduction

In this work, we present a neuroelectric system and examine its behaviour under different experimental conditions. The system is considered as a "black box" where the incoming information (input) modifies its behaviour and produces a response (output). The input and output processes are stochastic signals, which are called point processes [9,10,14,21] and denoted by N_1 and N_2, respectively (see Fig. 1).

The identification of the neuroelectric system, which is assumed to be stochastic and time invariant, will be based on the information contained in the input and output processes. Since our system is stochastic, complete identification is not possible and the best we can hope for is to find estimates of the parameters which characterise the statistical properties of the system [7].

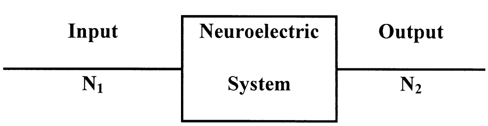

Fig. 1. A graphical representation of the neuroelectric system.

The estimation of the parameters of the system will be based on attractive methods of spectral analysis for point processes. Two important reasons that make the use of spectral analysis techniques in the analysis of point processes attractive are:

(a) it is much easier to obtain asymptotic results for the estimates of the parameters involved in the time and frequency domains;
(b) the computation of the estimates becomes faster with the use of the fast Fourier transform (FFT).

The importance of the second reason lies on the fact that the estimates of the time domain parameters can be rapidly obtained by first calculating the corresponding parameters in the frequency domain directly from the data and then inverting to the time domain. For the estimation of the spectral density functions, we shall use Welch's method based on the modified periodogram statistics. Since the procedure of estimation is based on the computation of the modified periodogram statistics, it is defined as non-parametric.

Two data sets from the field of Neurophysiology will be used in order to examine the behaviour of the neuroelectric system. The data sets describe the cases where the system:

(a) is free from any input;
(b) is affected by the presence of an input (alpha motoneuron).

2. Brief description of the neuroelectric system

The neuroelectric system that will be described is called "muscle spindle" and is an element of the peripheral neuromuscular system.

The muscle spindle is a receptor which is thought to play an important role in the initiation of movement and in the maintenance of posture. Muscle spindles respond to external stimuli and consist of parts of the "skeletal" muscles, which are concerned with posture or movement. Most "skeletal" muscles contain a number of these receptors, which lie in parallel with the "extrafusal fibres". They consist of a number of specialised muscle fibres lying parallel to each other and partially contained within a fluid-filled capsule of connective tissue [3]. The fibres of the muscle spindle known as "intrafusal fibres" are considerably shorter than the extrafusal muscle fibres.

A group of neurons, the "alpha motoneurons", whose bodies lie within the spinal cord, have long axons which leave the spinal cord to innervate the extrafusal muscle fibres forming the main mass of muscles responsible for generating forces or changes of length. The axons of alpha motoneurons normally conduct electric signals (nerve pulses) from the cell body to the extrafusal muscle fibres. When an electric signal reaches the junction between the axon and the muscle fibre, a sequence of electro-chemical events occurs which leads to the contraction of the extrafusal muscle fibres. The alpha motoneuron together with all of the muscle fibers that it innervates is called a 'motor-unit'. Skeletal muscles are thus, in part, made up of groups of motor-units. The size of a motor-unit (the number of muscle fibers innervated by a particular alpha motoneuron), and the number of motor-units within a muscle, depend on the function of that muscle.

Motor-units may be related to the incremental units of force that a muscle can develop. Muscles concerned with the control of delicate movements have small motor-units and can generate the small increments of force required for these movements, whereas muscle with large motor-units produce large increments of force and may function simply to maintain a fixed attitude or posture.

Our purpose in this work is to examine how the effect of an alpha motoneuron on the extrafusal fibres of a muscle affects the behaviour of a muscle spindle lying within the muscle by recording the response of the Ia sensory axon (the axon that conducts the information from the muscle spindle to the spinal cord). When the muscle is not affected by a stimulus, the Ia sensory axon from the muscle spindle generates electric signals at a constant rate. By changing the length of the muscle, we obtain a change in the rate of discharge of the electric signals in the Ia sensory axon [16].

The tenuissimus muscle in anaesthetised cats was used in the experiments, and the responses of single sensory axons in dorsal root filaments were recorded. The axon of the alpha motoneuron was stimulated by sequences of pulses at twice threshold having approximately an exponential distribution of intervals. By "threshold", we refer to the critical value over which a nerve impulse will occur. Fifteen seconds of responses were recorded when: (a) no stimulation was present and (b) an alpha stimulation was present, with the tenuissimus muscle held at a fixed length. The times of occurrence of the nerve impulses of the sensory axons and the stimulus pulses were measured and stored in computer files.

3. Theory of stationary point processes

Mathematically a point process $\{N(t)\}$ is defined as a random, non-negative, integer-valued measure [6]. Examples of point processes which are observed at a certain time interval are the failures of a computer, the beats of human heart, the action potentials fired by a neuron, the earthquakes that occur in a given region and many others.

In our practical problem, we shall assume that the point processes satisfy the following conditions:
(a) They are stationary.
(b) They are orderly.
(c) They are strong mixing.
These assumptions are discussed in detail in [7,10].

We now proceed to define some parameters for the point processes in both time and frequency domains.

Let $\{N_1(t), N_2(t)\}$, $-\infty < t < \infty$, be a bivariate point process. The mean intensity of component $N_k(t)$ $(k = 1{,}2)$ is defined by

$$p_k = \lim_{h\to 0} \text{Prob}\{\text{event of } k\text{-type occurs in } (t, t+h]\}/h. \quad (1)$$

The condition of orderliness implies that

$$E\{\mathrm{d}N_k(t)\} = p_k\,\mathrm{d}t, \quad (2)$$

where $\mathrm{d}N_k(t) = N_k(t, t+\mathrm{d}t]$ is the differential increment of $N_k(t)$, $k = 1{,}2$.

The second-order product density of the bivariate point process is defined by

$$p_{k\ell}(u) = \lim_{h_1,h_2\to 0} \text{Prob}\{\text{event of } k\text{-type occurs in } (t+u, t+u+h_1] \text{ and event of } \ell\text{-type occurs in } (t, t+h_2]\}/h_1h_2. \quad (3)$$

In this case, the condition of orderliness implies that

$$E\{\mathrm{d}N_k(t+u)\,\mathrm{d}N_\ell(t)\} = [p_{k\ell}(u) + p_k\,\mathrm{d}(u)\,\mathrm{d}\{k-\ell\}]\,\mathrm{d}u\,\mathrm{d}t, \quad (4)$$

where $\delta(.)$ is the dirac delta function and $\delta\{.\}$ is the Kronecker delta. Since the bivariate process is also strong mixing, it follows that

$$\lim_{u\to\infty} p_{k\ell}(u) = p_k p_\ell. \quad (5)$$

The covariance function between the increments $\mathrm{d}N_k(t+u)$ and $\mathrm{d}N_\ell(t)$ is defined by

$$\operatorname{cov}\{\mathrm{d}N_k(t+u), \mathrm{d}N_\ell(t)\} = [q_{k\ell}(u) + p_k\mathrm{d}(u)\mathrm{d}\{k-\ell\}]\,\mathrm{d}u\,\mathrm{d}t, \quad (6)$$

where $q_{k\ell}(u) = p_{k\ell}(u) - p_kp_\ell$ is the cumulant density.

In the frequency domain, we define the spectral density function as follows:

$$f_{k\ell}(\lambda) = (2\pi)^{-1}\int_{-\infty}^{+\infty} \exp\{-\mathrm{i}\lambda u\} \times \operatorname{cov}\{\mathrm{d}N_k(t+u), \mathrm{d}N_\ell(t)\}/\mathrm{d}t \quad (7)$$

provided that $\int_{-\infty}^{+\infty} |q_{k\ell}(u)|\,\mathrm{d}u < +\infty$. This definition implies that

$$\lim_{\lambda\to\infty} f_{k\ell}(\lambda) = \begin{cases} (2\pi)^{-1}p_k & k = \ell, \\ 0 & k \neq \ell. \end{cases} \quad (8)$$

The definitions of the power spectrum and the cross-spectrum for point processes follow from (7) when we let $k = \ell$ and $k \neq \ell$, respectively.

Another important function in the frequency domain is the coherence coefficient defined by

$$|R_{k\ell}(\lambda)|^2 = \frac{|f_{k\ell}(\lambda)|^2}{f_{kk}(\lambda)f_{\ell\ell}(\lambda)}, \quad (9)$$

where $f_{k\ell}(\lambda)$ is the cross-spectrum and $f_{kk}(\lambda)$, $f_{\ell\ell}(\lambda)$ are the power spectral densities of components N_k and N_ℓ of the bivariate process, respectively.

The coherence coefficient takes values in the interval [0,1] and provides a measure for the linear relationship between the components of the bivariate point process (more details about the parameters defined above can be found in [6,7,13]).

4. Estimates of the frequency domain parameters

In this section, we discuss estimates of the spectral density functions and the coherence coefficient.

An estimate of the spectral density, $f_{k\ell}(\lambda)$, may be based on Welch's method which uses the modified periodogram. A brief discussion of this method is as follows:

Suppose that the number of disjoint sections is L, each of length R, so that the total time interval is $T = LR$. The modified finite Fourier–Stieltjes transform of the increments $\mathrm{d}N_k(t)$ $(k = 1{,}2)$ for a section of length R is defined by

$$\hat{d}_k^{(R)}(\lambda, j) = \int_{jR}^{(j+1)R} \exp(-\mathrm{i}\lambda t)[\mathrm{d}N_k(t) - \hat{p}_k\,\mathrm{d}t], \quad j = 0,1,\ldots,L-1, \quad (10)$$

where $\hat{p}_k$ is the estimate of the mean intensity of the k-component. By subtracting the estimate of the mean intensity, we reduce the leakage near the frequency $\lambda = 0$.

The modified periodogram of a section of length R is now given by

$$\hat{I}_{k\ell}^{(R)}(\lambda, j) = (2\pi R)^{-1} \hat{d}_k^{(R)}(\lambda, j)\overline{\hat{d}_\ell^{(R)}(\lambda, j)}$$

$$\text{for } \lambda \neq 0 \text{ and } j = 0,1,\dots,L-1, \tag{11}$$

where $\overline{\hat{d}_\ell^{(R)}(\lambda, j)}$ is the conjugate function of $\hat{d}_\ell^{(R)}(\lambda, j)$.

In practice, in order to be able to use the FFT algorithm in the computation of the modified periodogram, we approximate (10) by the following expression:

$$\hat{d}_k^{(R)}(\lambda, j) \approx \sum_{t=jR}^{(j+1)R-1} \exp(-\mathrm{i}\lambda t)[N_k(t+1) - N_k(t) - \hat{p}_k]. \tag{12}$$

The estimate of the cross-spectrum $f_{k\ell}(\lambda)$ over the total time interval ($T = LR$) is now obtained by

$$f_{k\ell}^{(LR)}(\lambda) = L^{-1} \sum_{j=0}^{L-1} \hat{I}_{k\ell}^{(R)}(\lambda, j) \quad \text{for } \lambda \neq 0. \tag{13}$$

This estimate is asymptotically unbiased and its variance tends to zero for large L (more details about this method can be found in [20]). If the number of disjoint sections L is not large enough, we can improve the smoothness of the above estimate by using a weighting scheme of the form

$$\hat{f}_{k\ell}^{(LR)}(\lambda_m) = \frac{1}{2p+1} \sum_{r=-p}^{p} f_{k\ell}^{(LR)}(\lambda_{m+r}), \tag{14}$$

where $\lambda_m = 2\pi m/R$ and $m = 1,2,\dots,(R-1)/2$.

It is clear from (14) that the estimate for the cross-spectrum is obtained when $k \neq \ell$, while the estimate for the power spectrum when $k = \ell$ (in the case of ordinary time series these estimates can be found in [1,8,17]).

We next turn to the estimation of the coherence coefficient. By substituting the estimates of the cross-spectrum and the power spectra in (9) we get an estimate of the coherence coefficient given by

$$|\hat{R}_{k\ell}(\lambda)|^2 = \frac{|\hat{f}_{k\ell}^{(LR)}(\lambda)|^2}{\hat{f}_{kk}^{(LR)}(\lambda)\hat{f}_{\ell\ell}^{(LR)}(\lambda)} \quad \text{for } \lambda \neq 0 \ (k \neq \ell). \tag{15}$$

Under the null hypothesis $|R_{k\ell}(\lambda)|^2 = 0$, the distribution of $|\hat{R}_{k\ell}(\lambda)|^2$ is a beta distribution with 1 and $M-1$ degrees of freedom, where $M = (2p+1)L$ (see [8, p. 294]), p is a value that has to be chosen in order to obtain a consistent estimate of the power spectrum, i.e., one that has been satisfactory smoothed. By using the arguments of Abramowitz and Stegun [2, p. 944] we find

$$\mathrm{Prob}\{|\hat{R}_{k\ell}(\lambda)|^2 < z\} = 1 - (1-z)^{M-1},$$

$$0 < z < 1. \tag{16}$$

By setting $\alpha = \mathrm{Prob}\{|\hat{R}_{k\ell}(\lambda)|^2 < z\}$, we get from (16) the following expression:

$$z = 1 - (1-\alpha)^{1/(M-1)}. \tag{17}$$

When the values of $|\hat{R}_{k\ell}(\lambda)|^2$ are less than z, we cannot reject the null hypothesis. In this case we say that the components of the bivariate point process are uncorrelated.

5. System identification

In this section, we present a linear stochastic model which is suitable for the identification of the neuroelectric system, the muscle spindle. It is assumed that the muscle spindle is a time-invariant system with input process N_1 and output process N_2. A basic element characterising such a system is the conditional expected value $E\{\mathrm{d}N_2(t)/N_1\}$ interpreted as

Prob{there is event of type-2

in $(t, t+h]$/an event of type-1 at t}.

The stochastic model which describes the linear relationship between the input N_1 and the output N_2 is given by

$$E\{\mathrm{d}N_2(t)/N_1\} = \left[\mu + \int_{-\infty}^{t} a(t-u)\,\mathrm{d}N_1(t)\right]\mathrm{d}t. \tag{18}$$

This is a Volterra-type stochastic model for point processes (such models are discussed in [5,15]). The function $a(u)$ is called the impulse response function and is useful in predicting whether there will be an event of type-2 u time units away from a type-1 event, while μ is a constant representing the mean rate of process N_2, when N_1 is inactive.

In order to be able to solve model (18) with respect to the unknown parameters μ and $a(u)$, we need to use techniques of the frequency domain. For this reason, we define the one-sided Fourier transform of $a(u)$ as follows:

$$A(\lambda) = \int_0^{\infty} a(u) \exp(-\mathrm{i}\lambda u)\,\mathrm{d}u, \quad -\infty < \lambda < \infty. \tag{19}$$

It follows from (18) after some calculations, that

$$p_2 = \mu + A(0)p_1 \tag{20}$$

and

$$A(\lambda) = f_{21}(\lambda)/f_{11}(\lambda) \tag{21}$$

provided that $f_{11}(\lambda) \neq 0$. For more details refer to Brillinger [5]. By p_1 and p_2, we denote the mean intensities of N_1 and N_2, respectively. The function $A(\lambda)$ is a complex function and can be described by the magnitude $|A(\lambda)|$ and the phase $\theta(\lambda)$.

The function $a(u)$ can be determined by using the inverse Fourier transform of (19), that is

$$a(u) = (2\pi)^{-1} \int_{-\infty}^{+\infty} A(\lambda) \exp(\mathrm{i}\lambda u)\,\mathrm{d}\lambda. \tag{22}$$

The parameter μ can also be determined from (20).

Estimates for the parameters $|A(\lambda)|$, $\theta(\lambda)$, μ and $a(u)$ are now obtained as follows:

$$|\hat{A}(\lambda)| = |\hat{f}_{21}^{(LR)}(\lambda)|/\hat{f}_{11}^{(LR)}(\lambda), \tag{23}$$

$$\hat{\theta}(\lambda) = \arg \hat{f}_{21}^{(LR)}(\lambda), \tag{24}$$

$$\hat{\mu} = \hat{p}_2 - \hat{A}(0)\hat{p}_1 \tag{25}$$

and

$$\hat{a}(u) = Q_R^{-1} \sum_k W_R(\lambda_k) \hat{A}(\lambda_k) \exp(\mathrm{i}\lambda_k u),$$
$$k = 0, \pm 1, \pm 2, \ldots, \pm (Q_R - 1)/2, \tag{26}$$

where $W_R(\lambda) = W(b_R \lambda)$ is a convergence factor and $\lambda_k = 2\pi k/Q_R$. Q_R is a quantity that satisfies the condition $b_R Q_R \to \infty$. By b_R, we denote the bandwidth which tends to zero as $R \to \infty$ (more details about the convergence factors and their properties can be found in [11]). Statistical methods concerning the estimation of the parameters given by (23)–(26) are discussed in [4]. Our approach here is based on Welch's method which can be used to develop some new asymptotic results for the estimates $\log_{10}|\hat{A}(\lambda)|$, $\hat{\theta}(\lambda)$ and $\hat{a}(u)$.

Proposition 1. *Let $\{N_1(t), N_2(t)\}$ be a stationary point process defined on $(0, T]$. Suppose that the point process is strong mixing and its moments exist up to the Jth order. Then, if $f_{11}(\lambda) \neq 0$, the estimate $\log_{10}|\hat{A}(\lambda)|$ is asymptotically unbiased and its variance is given by*

$$\mathrm{Var}\{\log_{10}|\hat{A}(\lambda)|\}$$
$$\cong \frac{(\log_{10} e)^2}{2(2p+1)L} f_{22}(\lambda) f_{11}^{-1}(\lambda)[|R_{21}(\lambda)|^{-2} - 1],$$
$$\lambda \neq 0,$$

where e is the base of the natural logarithm.

Proposition 2. *Suppose that the conditions of Proposition 1 are satisfied. Then the estimate $\hat{\theta}(\lambda)$ is asymptotically unbiased and its variance is given by*

$$\mathrm{Var}\{\hat{\theta}(\lambda)\} \cong \frac{[1 - \delta\{2\lambda\}]}{2(2p+1)L}[|R_{21}(\lambda)|^{-2} - 1].$$

Theorem 1. *We suppose that the conditions of Proposition 1 are satisfied and $\int |u|\,|a(u)|\,\mathrm{d}u < +\infty$. Then, if $b_R Q_R \to \infty$ as $R \to \infty$, the distribution of $\hat{a}(u)$ is approximately normal with mean $a(u)$ and variance given by*

$$\mathrm{Var}\{\hat{a}(u)\} \cong \frac{(2\pi)^{-1}}{(2p+1)LQ_R}$$
$$\int W_R^2(\lambda) f_{22}(\lambda) f_{11}^{-1}(\lambda)[1 - |R_{21}(\lambda)|^2]\,\mathrm{d}\lambda.$$

Proposition 1 and Theorem 1 are used to develop the asymptotic properties of $\hat{a}(u)$, from which we can obtain its confidence limits. Propositions 1 and 2 show that the variance of $\log_{10}|\hat{A}(\lambda)|$ and $\hat{\theta}(\lambda)$ depends on $|R_{21}(\lambda)|^{-2}$, respectively. This indicates that the behaviour of $\log_{10}|\hat{A}(\lambda)|$ and $\hat{\theta}(\lambda)$ will be very irregular when the estimate of $|R_{21}(\lambda)|^{-2}$ is close to zero. The proofs of the two propositions and the theorem are included in the appendix.

The theoretical results for the estimated parameters of the Volterra-type model obtained from the estimates of the spectral density functions will help us to extract useful conclusions about the behaviour of the muscle spindle in relation to the information which is carried to spinal cord through the Ia sensory axon of the muscle spindle.

6. Examples

In this section, we analyse the response of the neuroelectric system when : (a) it is not affected by any stimulus (spontaneous activity) and (b) it is affected by an alpha motoneuron.

Fig. 2 shows the logarithm to base 10 of the estimate of the power spectrum ($\log_{10}\{$power spectrum$\}$) of the response of the neuroelectric system in the case (a) computed from (14) by setting $k = \ell$, number of disjoint sections $L = 5$, each of length $R = 2048$ and $p = 15$. It is obvious from the figure that the behaviour of the response is periodic which suggests that the distances between the events of the response are almost equal. It is also apparent that the true value of $\log_{10}\{$power spectrum$\}$ tends to the constant value $\log_{10}\{(2\pi)^{-1}p_k\}$ as λ (angular frequency) becomes larger according to (8). The dashed line in the middle corresponds to the estimate $\log_{10}\{(2\pi)^{-1}\hat{p}_k\}$, where $\hat{p}_k$ is the estimate of the mean intensity of the response. The solid lines above and below the dashed line correspond to the 95% confidence limits, the computation of which is discussed in Rigas [18]. Values of the estimated $\log_{10}\{$power spectrum$\}$ inside the 95% confidence limits indicate a completely random point process (i.e., a Poisson process).

Fig. 3 shows the logarithm to base 10 of the estimate of the power spectrum of the response when the muscle spindle is affected by the presence of an alpha motoneuron (case (b)), which is computed in the same way as discussed above. In this case, the estimate $\hat{p}_k$ corresponds to the mean intensity of the response of the neuroelectric system in

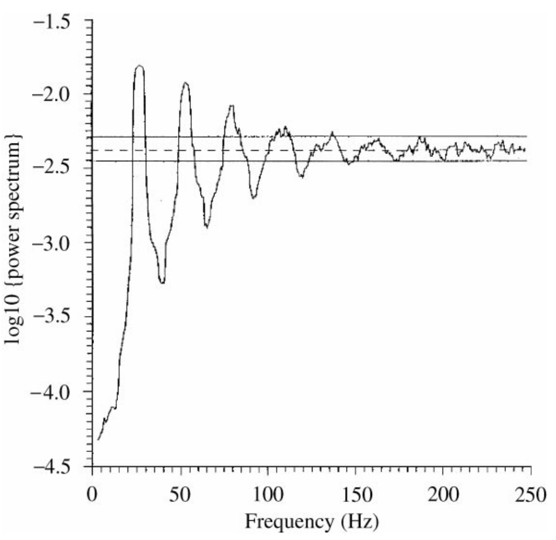

Fig. 2. Estimate of the logarithm to base 10 of the power spectrum of the response of the neuroelectric system when it is not affected by any stimulus (spontaneous activity).

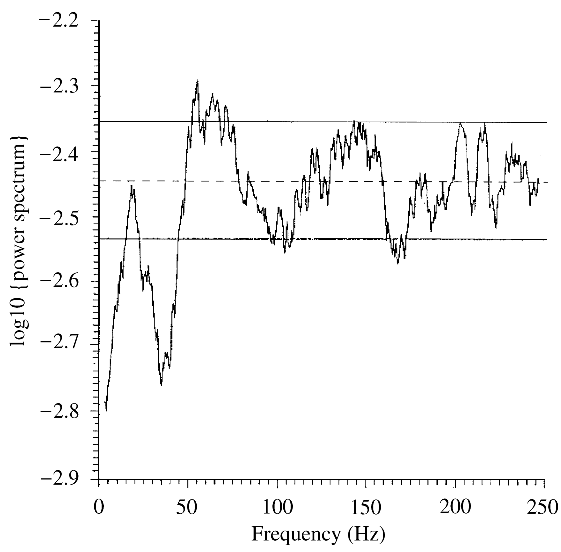

Fig. 3. Estimate of the logarithm to base 10 of the power spectrum of the response of the neuroelectric system when an alpha motoneuron is present.

the presence of an alpha motoneuron. The $\log_{10}\{\text{power spectrum}\}$ is low almost in the whole range of frequencies 0–50 Hz and high (higher than a completely random process) in the range 50–70 Hz. A peak at about 26 Hz and its multiple at 55 Hz suggest the presence of spontaneous activity. Hence, we may say that the system behaves as a high-pass filter, since it permits mostly high-frequency components to pass through in the range of frequencies 0–70 Hz.

Fig. 4 illustrates the estimate of the coherence coefficient between the effect of the alpha motoneuron and the response of the neuroelectric system. The dashed line indicates the 95% point of the estimate of the coherence coefficient computed from (17) for $M = 155$. The two processes are more strongly related at low frequencies with a weaker relation until 100 Hz.

Fig. 5 shows the estimate of the gain or $\log_{10}|\hat{A}(\lambda)|$ and is plotted until 25 Hz, since the estimate of the coherence coefficient becomes relatively small at around this frequency. The shape of the graph shows an increase in the gain with a maximum between 15 and 20 Hz. After that there is clearly a decrease in the gain. From this result we may conclude that the system behaves as a band-pass filter in the range of frequencies 1–25 Hz.

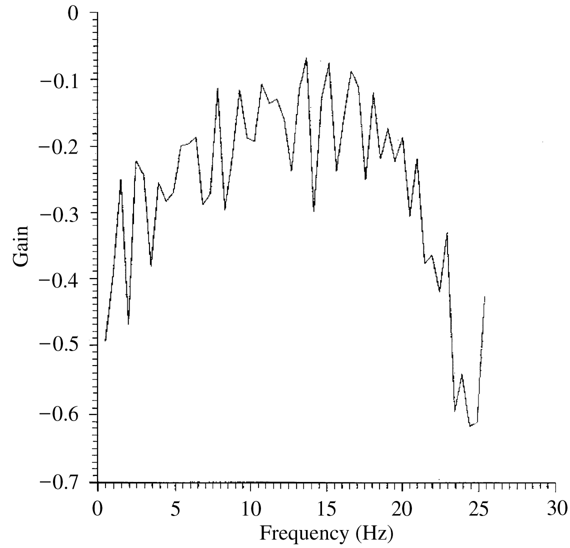

Fig. 5. Estimate of the gain of the neuroelectric system when it is affected by an alpha motoneuron.

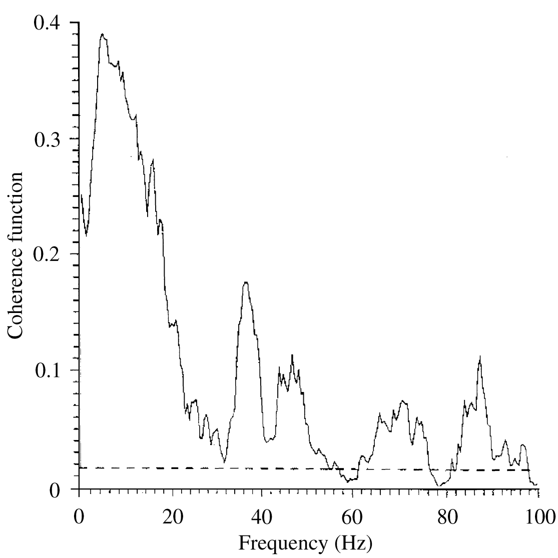

Fig. 4. Estimate of the coherence coefficient in the case where the neuroelectric system is affected by an alpha motoneuron.

Fig. 6 provides the estimate of the phase. The phase characteristic is compatible with a linear phase lead feature in the system (see [12, p. 23]). This is also supported by the initial gain increase from 0 to 8 Hz. The phase starts at about -3.14 and is a straight line with increasing values. This indicates that the system is delayed for about 30 ms. This value is obtained from the formula $\lambda_c = \pi/u$ (see [8, p. 303]), with $\lambda_c = 2\pi f_c$ and $f_c = 15.4$ Hz is the frequency which corresponds to the point where the estimate of the phase meets the axis that passes from zero and is parallel to the axis of the frequencies. From the above formula, we calculate the delay u to be approximately 32.5 ms.

Fig. 7 depicts the estimate of the impulse response function. The impulse response function for our stochastic system can be interpreted as a best linear predictor showing whether there will be an event of type-2 u time units away from an event of type-1. The dashed line in the middle corresponds to the hypothesis that the two processes (input and output) are independent and the solid lines give the 95% confidence limits for the estimate of the

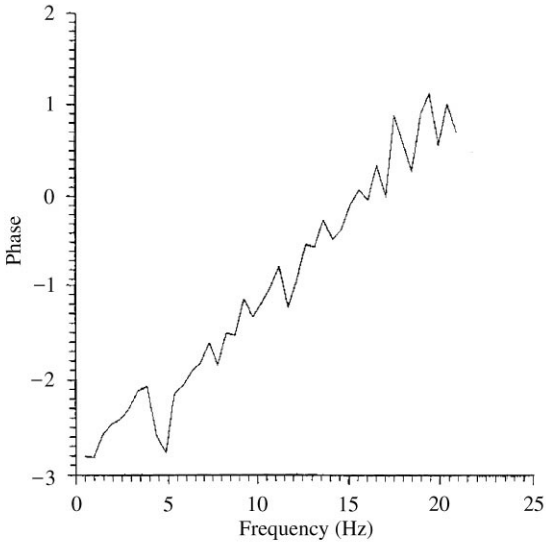

Fig. 6. Estimate of the phase when the neuroelectric system is affected by an alpha motoneuron.

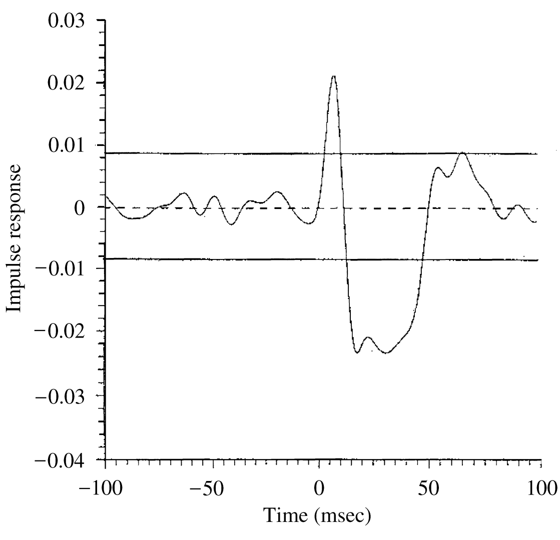

Fig. 7. Estimate of the impulse response function of the neuroelectric system.

impulse function. Values of the estimate outside the confidence limits indicate deviations from the hypothesis that the two processes are independent. The solid lines are obtained from the expression $\pm 2\sqrt{s}$, where

$$s = \frac{1}{MQ_R^2} \sum_k W_R^2(\lambda_k) \hat{f}_{22}(\lambda_k) \hat{f}_{11}(\lambda_k)[1 - |\hat{R}_{21}(\lambda_k)|^2],$$

$$k = 0, \pm 1, \pm 2, \ldots, \pm^{(Q_R - 1)/2}.$$

A Parzen convergence factor $W_R(\lambda)$ was used to smooth the estimate of the impulse response, with $b_R^{-1} = 30$ and $Q_R = 256$.

The impulse response function can be positive, negative or zero, depending on whether the response of the system accelerates, slows or remains unchanged, respectively. From Fig. 7, it becomes clear that the system responds (accelerates) for a short time period of 1–2 ms, then slows (its response is in a way blocked) for about 30 ms and after that the response does not change.

7. Conclusions

In this paper, we have studied the behaviour of the neuroelectric system called "muscle spindle", under the influence of an alpha motoneuron using a stochastic model of Volterra-type for stationary point processes. The estimates for the parameters of the stochastic model are obtained from the estimates of the spectral density functions which are based on Welch's method.

Two main results were found:

(A) The effect of the alpha motoneuron modifies completely the behaviour of the system which acts almost as a high-pass filter, according to the estimate of the power spectrum of the response.

(B) The system accelerates for 1–2 ms very shortly after the effect of the alpha motoneuron, slows down (the response is in a way blocked) for about 30 ms and after that does not change according to the estimate of the impulse response function.

The effect of the alpha motoneuron makes the muscle to contract and this in a way blocks the transmission of the information from the muscle spindle to the spinal cord through the Ia sensory axon. This result is considerably different, when compared to the effect of a gamma motoneuron [19]. The effect of a gamma motoneuron makes the system only to accelerate for about 5–10 ms after a delay in the response of about 15 ms. Future research will consider the combined effect of an alpha and a gamma motoneuron on the muscle spindle using Volterra-type stochastic models.

Acknowledgements

The authors are most grateful to Professor G.R. Moore and Professor J.R. Rosenberg for providing the data sets. We would also like to thank Professor Peter Wellstead for the helpful discussions and suggestions.

Appendix. Proofs of asymptotic results

Proof of Proposition 1. We start by examining the asymptotic first- and second- order properties of $A(\lambda)$.

Using the results of Brillinger [5], we can write the estimate of the transfer function obtained from (21) in the following form:

$$\hat{A}(\lambda) = \mathrm{A}(\lambda) + \frac{[\hat{f}^{(LR)}_{21}(\lambda) - f_{21}(\lambda)]}{f_{11}(\lambda)}$$

$$- \frac{A(\lambda)}{f_{11}(\lambda)}[\hat{f}^{(LR)}_{11}(\lambda) - f_{11}(\lambda)] + \mathrm{O_p}\{(MR)^{-1/2}\},$$

where $\mathrm{O_p}\{(MR)^{-1/2}\}$ indicates probability of order $\mathrm{O}\{(MR)^{-1/2}\}$ [8, p. 423].

From this relation and the properties of the estimates $\hat{f}^{(LR)}_{k\ell}(\lambda)$ [20], we obtain

$$\lim_{R\to\infty} E\{\hat{A}(\lambda)\} = A(\lambda)$$

and

$$\lim_{R\to\infty} \mathrm{cov}\{\hat{A}(\lambda),\hat{A}(\mu)\}$$

$$= \frac{\delta\{\lambda-\mu\}}{(2p+1)L}\left[\frac{f_{22}\lambda}{f_{11}\lambda} - \frac{f_{21}(\lambda)f_{21}(-\mu)}{f^2_{11}(\mu)}\right] \quad (\lambda \neq \mu).$$

These asymptotic results will be extensively used in the proofs below.

In order to find the properties of $\log_{10}|\hat{A}(\lambda)|$ we use the following first-order Taylor expansion

$$\ln|\delta+\varepsilon| = \ln|\delta| + \frac{1}{2}\left(\frac{\varepsilon}{\delta} + \frac{\bar{\varepsilon}}{\bar{\delta}}\right) - \cdots,$$

where ε is assumed to be small and $\bar{\varepsilon}$ denotes the conjugate of ε. By setting $\delta = A(\lambda)$ and $\delta + \varepsilon = \hat{A}(\lambda)$ we get

$$\ln|\hat{A}(\lambda)| = \ln|A(\lambda)| + \frac{1}{2}\frac{[\hat{A}(\lambda) - A(\lambda)]}{A(\lambda)}$$

$$+ \frac{1}{2}\frac{[\hat{A}(-\lambda) - A(-\lambda)]}{A(-\lambda)} - \cdots,$$

where $\overline{A(\lambda)} = A(-\lambda)$ since $A(\lambda)$ is a complex function. This relation leads to the asymptotic results

$$\lim_{R\to\infty} E\{\ln|\hat{A}(\lambda)|\} = \ln|A(\lambda)|,$$

$$\lim_{R\to\infty} \mathrm{cov}\{\ln|\hat{A}(\lambda)|,\ln|\hat{A}(\mu)|\}$$

$$= \frac{\delta\{\lambda-\mu\}}{2(2p+1)L}\frac{1}{A(\lambda)A(-\mu)}$$

$$\times\left[\frac{f_{22}(\lambda)}{f_{11}(\lambda)} - \frac{f_{21}(\lambda)f_{21}(-\mu)}{f_{11}{}^2(\mu)}\right] \quad (\lambda \neq \mu).$$

In the previous relation, if we set $\lambda = \mu$ and use the fact that $\ln|\hat{A}(\lambda)| = \log_{10}|\hat{A}(\lambda)|/\log_{10} e$, we get

$$\mathrm{Var}\{\log_{10}|\hat{A}(\lambda)|\}$$

$$\cong \frac{(\log_{10} e)^2}{2(2p+1)L} f_{22}(\lambda) f_{11}^{-1}(\lambda)[|R_{21}(\lambda)|^{-2} - 1],$$

$$\lambda \neq 0.$$

This completes the proof of the proposition. □

Proof of Proposition 2. In order to prove the asymptotic results of the estimate of the phase, the following first-order Taylor expansion may be used:

$$\arg\{\delta+\varepsilon\} = \arg\delta + \arg\left\{\left(1 + \frac{\varepsilon}{\delta}\right)\right\}$$

$$= \arg\delta + \frac{1}{2i}\left(\frac{\varepsilon}{\delta} - \frac{\bar{\varepsilon}}{\bar{\delta}}\right) - \cdots.$$

By setting $\delta + \varepsilon = \hat{f}_{21}^{(LR)}(\lambda)$ and $\delta = f_{21}(\lambda)$ we obtain

$$\arg\hat{f}_{21}^{(LR)}(\lambda) = \arg f_{21}(\lambda) + \frac{1}{2i}\left[\frac{\hat{f}_{21}^{(LR)}(\lambda) - f_{21}(\lambda)}{f_{21}(\lambda)}\right] - \frac{1}{2i}\left[\frac{\hat{f}_{21}^{(LR)}(-\lambda) - f_{21}(-\lambda)}{f_{21}(-\lambda)}\right] - \dots,$$

where $\overline{f_{21}(\lambda)} = f_{21}(-\lambda)$, since $f_{21}(\lambda)$ is a complex function.

Now it can be shown that $\hat{\theta}(\lambda)$ is asymptotically unbiased and its variance is given by

$$\mathrm{Var}\{\hat{\vartheta}(\lambda)\} \cong \frac{[1-\delta\{2\lambda\}]}{2(2p+1)L}[|R_{21}(\lambda)|^{-2} - 1].$$

This indicates a simple way of proving the results of the proposition. For further details, refer to Priestley [17, p. 703].

Proof of Theorem 1. If we take the expected value in (26) we have

$$\begin{aligned} E\{\hat{a}(u)\} &= Q_R^{-1}\sum_k W_R(\lambda_k)E\{\hat{A}(\lambda_k)\}\exp\{\mathrm{i}\lambda_k u\} \\ &= Q_R^{-1}\sum_k W_R(\lambda_k)A(\lambda_k)\exp\{\mathrm{i}\lambda_k u\} + \mathrm{O}\{(MR)^{-1}\} \\ &= (2\pi)^{-1}\int W(b_R\lambda)A(\lambda)\exp\{\mathrm{i}\lambda u\}\,\mathrm{d}\lambda + \mathrm{O}\{Q_R^{-1}\} + \mathrm{O}\{(MR)^{-1}\} \end{aligned}$$

and

$$\lim_{R\to\infty} E\{\hat{a}(u)\} = 2\pi\int A(\lambda)\exp\{\mathrm{i}\lambda u\}\,\mathrm{d}\lambda = a(u),$$

since, as $R \to \infty$, $Q_R \to \infty$ and $b_R \to 0$. In the above expression, $W_R(\lambda) = W(b_R\lambda)$ is a convergence factor, Q_R satisfies $b_R Q_R \to \infty$ and b_R is the bandwidth. This implies that $W(b_R\lambda) \to W(0) = 1$.

For the covariance of $\hat{a}(u)$ and $\hat{a}(v)$ we have

$$\begin{aligned} &\mathrm{cov}\{\hat{a}(u),\hat{a}(v)\} \\ &= Q_R^{-2}\sum_k\sum_\ell W_R(\lambda_k)W_R(\mu_\ell)\,\mathrm{cov}\{\hat{A}(\lambda_k),\hat{A}(\mu_\ell)\}\exp\{\mathrm{i}(\lambda_k u - \mu_\ell v)\} \\ &= Q_R^{-2}\sum_k\sum_\ell W_R(\lambda_k)W(\mu_\ell)\frac{\delta\{\lambda_k - \mu_\ell\}}{(2p+1)L}\left[\frac{f_{22}(\lambda_k)}{f_{11}(\lambda_k)} - \frac{f_{21}(\lambda_k)f_{21}(-\mu_\ell)}{f_{11}^2(\mu_\ell)}\right]\exp\{\mathrm{i}(\lambda_k u - \mu_\ell v)\} \\ &= \frac{Q_R^{-2}}{(2p+1)L}\sum_k W_R^2(\lambda_k)f_{22}(\lambda_k)f_{11}^{-1}(\lambda_k) \times [1 - |R_{21}(\lambda_k)|^2]\exp\{\mathrm{i}\lambda_k(u-v)\} + \mathrm{O}(Q_R^{-1}M^{-1}R^{-1}) \\ &= \frac{(2\pi)^{-1}}{(2p+1)LQ_R}\int W_R^2(\lambda)f_{22}(\lambda)f_{11}^{-1}(\lambda) \times [1 - |R_{21}(\lambda)|^2]\exp\{\mathrm{i}\lambda(u-v)\}\,\mathrm{d}\lambda + \mathrm{O}(M^{-1}Q_R^{-2}) + \mathrm{O}(M^{-1}Q_R^{-1}R^{-1}). \end{aligned}$$

By setting $u = v$, we obtain the following result for the variance of $\hat{a}(u)$:

$$\mathrm{Var}\{\hat{a}(u)\} \cong \frac{(2\pi)^{-1}}{(2p+1)LQ_R} \times \int W_R^2(\lambda)f_{22}(\lambda)f_{11}^{-1}(\lambda)[1 - |R_{21}(\lambda)|^2]\,\mathrm{d}\lambda.$$

Higher-order cumulants are given by

$$\mathrm{cum}\{\hat{a}(u_1),\hat{a}(u_2),\dots,\hat{a}(u_J)\} = \mathrm{O}(M^{-J+1}Q_R^{-J+1}).$$

This result follows from the properties of the cumulants of the periodogram [8, p. 437].

Hence, the normalised cumulants can be written in the form

$$(MQ_R)^J\mathrm{cum}\{\hat{a}(u_1),\hat{a}(u_2),\dots,\hat{a}(u_J)\} = \mathrm{O}(M^{-J/2+1}Q_R^{-J/2+1}).$$

This further implies that

$$(MQ_R)^J\mathrm{cum}\{\hat{a}_1(u_1),\hat{a}_2(u_2),\dots,\hat{a}(u_J)\} \to 0$$

as $R \to \infty$ for $J > 2$.

From the last result we obtain that the distribution of $\hat{a}(u)$ is asymptotically normal (see [8, p. 403]).

References

[1] Special issue on spectral estimation, Proc. IEEE 70 (1982) 883–1125.

[2] M. Abramowitz, I.A. Stegun, Handbook of Mathematical Functions, National Bureau of Standards, Washington, 1964.

[3] I.A. Boyd, The isolated mammalian muscle spindle, Trends Neurosci. 3 (1980) 258–265.

[4] D.R. Brillinger, Cross-spectral analysis of processes with stationary increments including the stationary $G/G/\infty$ queue, Ann. Prob. 2 (1974) 815–827.

[5] D.R. Brillinger, Fourier analysis of stationary processes, Proc. IEEE 62 (1974) 1628–1643.

[6] D.R. Brillinger, Estimation of product densities, Proceedings of the Eighth Annual Symposium Interface of Computer Science and Statistics, Los Angeles, USA, 1975, pp. 431–438.

[7] D.R. Brillinger, The identification of point process systems, Ann. Prob. 3 (1975) 909–929.

[8] D.R. Brillinger, Time Series: Data Analysis and Theory, Expanded edition, Holden-Day, San Francisco, 1981.

[9] D.R. Cox, V. Isham, Point Processes, Chapman & Hall, London, 1980.

[10] D.J. Daley, D. Vere-Jones, An Introduction to the Theory of Point Processes, Spinger, Berlin, 1988.

[11] F.J. Harries, On the use of windows for harmonic analysis with the discrete transform, Proc. IEEE 66 (1978) 52–83.

[12] G.M. Jenkins, A survey of spectral analysis, Appl. Stat. 14 (1965) 2–32.

[13] P.A.W. Lewis, Remarks on the theory, computation and application of the spectral analysis of series of events, J. Sound Vib. 12 (1970) 353–375.

[14] P.A.W. Lewis (Ed.), Stochastic Point Processes, Wiley, New York, 1972.

[15] P.Z. Marmarelis, V.Z. Marmarelis, Analysis of Physiological Systems, Plenum Press, New York, 1978.

[16] P.B.C. Matthews, R.B. Stein, The regularity of primary and secondary muscle spindle afferent discharges, J. Physiol. 202 (1969) 59–82.

[17] M.B. Priestley, Spectral Analysis and Time Series, Academic Press, New York, 1981.

[18] A.G. Rigas, Spectral analysis of stationary point processes using the fast Fourier transform algorithm, J. Time Series Anal. 13 (5) (1992) 441–450.

[19] A.G. Rigas, Stochastic modeling of a complex physiological system, Proceedings of the International Conference on Differential Equations and their Applications to Biology and Industry, World Scientific, Singapore, 1996, pp. 409–415.

[20] A.G. Rigas, Spectral analysis of a stationary bivariate point process with applications to Neurophysiological problems, J. Time Series Anal. 17 (2) (1996) 171–187.

[21] W.A. Thompson Jr., Point Process Models with Applications to Safety and Reliability, Chapman & Hall, New York, 1988.